International Journal of Pharmaceutics 385 (2010) 150–156

Contents lists available at ScienceDirect

International Journal of Pharmaceutics

journal homepage: www.elsevier.com/locate/ijpharm

Pharmaceutical Nanotechnology

LyP-1-conjugated nanoparticles for targeting drug delivery to lymphatic metastatic tumors

Guopei Luo[a], Xianjun Yu[a,*], Chen Jin[a], Feng Yang[a], Deliang Fu[a], Jiang Long[a], Jin Xu[a], Changyou Zhan[b], Weiyue Lu[b]

[a] Pancreatic Disease Institute, Department of General Surgery, Huashan Hospital, Fudan University, Shanghai 200040, China
[b] Department of Pharmaceutics, School of Pharmacy, Fudan University, Shanghai 200032, China

ARTICLE INFO

Article history:
Received 24 June 2009
Received in revised form
11 September 2009
Accepted 4 October 2009
Available online 13 October 2009

Keywords:
PLGA
PEG
Nanoparticle
Targeting
Drug delivery
Tumor
Lymph metastasis

ABSTRACT

Active tumor targeting by biodegradable nanoparticles has been widely studied for cancer diagnosis and therapy. However, target-specific nanoparticles for drug delivery to lymphatic metastases have not been reported yet due to the lack of specific markers in the tumor lymphatics. Recently, peptide LyP-1 has been recognized for its specific home to tumors and their lymphatics. In this study, we tested the possibility of LyP-1 serving as a target-specific peptide of PEG–PLGA nanoparticles to tumor lymph metastases. LyP-1 was synthesized by using Boc-protected amino acids. The copolymers of maleimide–PEG–PLGA were formed by the conjugation of maleimide–PEG–NH_2 to PLGA–COOH, which were applied to prepare pegylated nanoparticles with mPEG–PLGA by means of double emulsion/solvent evaporation technique. LyP-1 with sulfhydryl group was conjugated to the maleimide function located at the distal end of PEG surrounding the nanoparticle surface. LyP-1-conjugated PEG–PLGA nanoparticle (LyP-1-NPs) had a round and regular shape with a diameter around 90 nm. *In vitro*, cellular uptake of LyP-1-NPs was about four times of that of PEG–PLGA nanoparticles without LyP-1 (NPs). *In vivo*, the uptake of LyP-1-NPs in metastasis lymph nodes was about eight times of that of NPs. This study indicates that LyP-1-NP is a promising carrier for target-specific drug delivery to lymphatic metastatic tumors.

1. Introduction

As to many carcinomas, lymphatic metastasis occurs extensively, which leads to frequent tumor relapse even after extended lymphadenectomy. The inability to remove all the lymph metastasis remains the primary cause of cancer death (Pepper, 2001; Van Trappen and Pepper, 2002). Chemotherapy involves the use of powerful drugs to kill malignant cells. However, systemic delivery of chemotherapeutic agents often fails to make drug concentration high enough to eradicate all the metastatic lesions. Accordingly, targeting drug delivery specific to lymphatic metastatic lesions holds great promise in minimizing systemic drug exposure and maximizing the therapeutic efficacy of the drug (Reddy et al., 2006).

Liposomes have been proposed as carriers for the delivery of therapeutic and diagnostic agents to the lymphatic system (Oussoren and Storm, 2001). Nevertheless, researchers found that after a subcutaneous injection, approximately 50% of the injected dose of liposomes was cleared from the injection site into the lymphatic vessels, and only 1–2% of these liposomes were retained in each draining lymph node (Agarwal et al., 2008; Oussoren and Storm, 2001; Phillips et al., 2000). Thus, great attempts have been made on increasing the deposition of drug carriers into lymph nodes.

Recently, numerous investigations have been concentrated on biodegradable nanoparticles for anti-cancer drug delivery, which has great potential to revolutionise the future of cancer therapy (Brannon-Peppas and Blanchette, 2004; Cheng et al., 2007; Farokhzad et al., 2006; Garinot et al., 2007; Gu et al., 2008; Okada et al., 1988; Oussoren and Storm, 2001; Soppimath et al., 2001; Townsend et al., 2007). As effective drug delivery devices, biodegradable polymeric nanoparticles were known for their high efficiency, biocompatibility and controlled releasing ability (Okada et al., 1988; Soppimath et al., 2001). Active targeting nanoparticle, which involves the use of peripherally conjugated targeting moieties to enhance the ability of direct delivery a therapeutic agent to a targeting site, would minimize systemic drug exposure and provide the potential for increasing the therapeutic efficiency and reducing multi-drug resistance (Reddy et al., 2006). However, due to the relatively lagging development of specific markers of tumors lymphatics, active targeting by biodegradable nanoparticles to lymphatic metastases has not been reported yet.

Abbreviations: NP, PEG–PLGA nanoparticle without LyP-1 conjugation; LyP-1-NP, LyP-1-conjugated PEG–PLGA nanoparticle.

* Corresponding author.
E-mail address: yuxianjun88@hotmail.com (X. Yu).

0378-5173/$ – see front matter © 2009 Elsevier B.V. All rights reserved.
doi:10.1016/j.ijpharm.2009.10.014

LyP-1 is a 9-amino-acid cyclic peptide identified by *in vivo* phage display technology on the MDA-MB-435 human carcinoma xenograft tumors (Laakkonen et al., 2002). Fluorescein-labeled LyP-1 can accumulate in structures identified as lymphatic vessels and also in tumor cells within hypoxic areas, but not in the blood vessel after an intravenous injection (Laakkonen et al., 2002, 2004). This peptide also homes to the metastatic lesions of tumors (Laakkonen et al., 2004). Therefore, it may serve as a good nanoparticle specific targeting moiety for lymphatic active drug delivery.

With these considerations, the purpose of this study is to synthesize LyP-1-NPs (Fig. 1) and examine the possibility of LyP-1-NP serving as a novel targeting drug carrier to lymphatic metastatic tumors.

2. Materials and methods

2.1. Materials

Maleimide–PEG–NH_2 (3500 MW) was obtained from Jenkem (Beijing, China); mPEG–PLGA (75:25, 34 kDa MW) and PLGA–COOH (34 kDa MW) were purchased from Daisheng (Ji'nan, China); N-hydroxysuccinimide (NHS) was from Medpep Co. Ltd. (Shanghai, China); dicyclohexylcarbodiimide (DCC) was from Sinopharm Chemcial Reagent Co. Ltd. (Shanghai, China); amino acids was purchased from Kabushiki Kaisha (Japan); peptide synthetic resin was from Fluka (Switzerland); O-benzotriazole-N,N,N′,N′-tetramethyl-uronium-hexafluorophosphate (HBTU) was obtained from American Bioanalytical (USA); N,N-diisopropylethylamine (DIPEA) was from Zillion Pharmaceuticals (Shanghai, China); sodium cholate was purchased from Sigma–Aldrich (China); fluorescent dyes including 6-coumarin and fluorescein isothiocyanate (FITC) were from Sigma–Aldrich (St. Louis, MO); fetal bovine serum (FBS) was purchased from Life Technologies/Invitrogen (Carlsbad, CA); RPMI-1640 media was from Gibco BRL (USA); double-distilled water was purified using a Millipore Simplicity System (Millipore, Bedford, MA). All chemicals were analytic reagent grades and used without further purification.

Human pancreatic cancer cell line BxPC-3 was obtained from Shanghai Institutes for Biological Science (China). The nude nu/nu BALB/c mice (SLACCAS, Shanghai, China) used in this study were treated according to protocols approved by the ethical committee of Fudan University and in compliance with NIH's Principles of Laboratory Animal Care.

2.2. Peptides synthesis

LyP-1 peptide (H-Cys^1-Cys^2-Gly^3-Asn^4-Lys^5-Arg^6-Thr^7-Arg^8-Gly^9-Cys^{10}-OH) was synthesized by using Boc-protected amino acids. HBTU was used as a coupling reagent in dimethylformamide activated with diisopropylethylamine. Peptides were amide-capped at the C terminus by the use of PAM resin. In order to form cyclic peptide after being connected to nanoparticles, the thiol of Cys^2 and Cys^{10} was protected by the acetamidomethyl (Acm), which could conjugate with each other during deprotection process. Cyclic LyP-1 was also synthesized by Acm deprotection at Cys^2 and Cys^{10} using iodine reagent for testing the binding affinity of cyclic to BxPC-3 cells. The peptide was purified by HPLC (Shimadzu, Japan), and the sequence was confirmed by mass spectrometry (ESI-MS).

2.3. Examination of LyP-1s binding affinity to BxPC-3 cells

LyP-1 was conjugated with FITC to test the binding affinity of LyP-1 to BxPC-3 cells. Ten milligrams of LyP-1 were dissolved in PBS (10 mg/mL, pH 8.0) and incubated with 5 mg FITC under gentle stirring at RT. The reaction was stirred for 4 h followed by the addition of 3-aminepropanol (250 μL) to combine the unreactive FITC. Reacted product was collected using a Zeba™ Desalt Spin Columns (Waters, USA), according to manufacturer's directions.

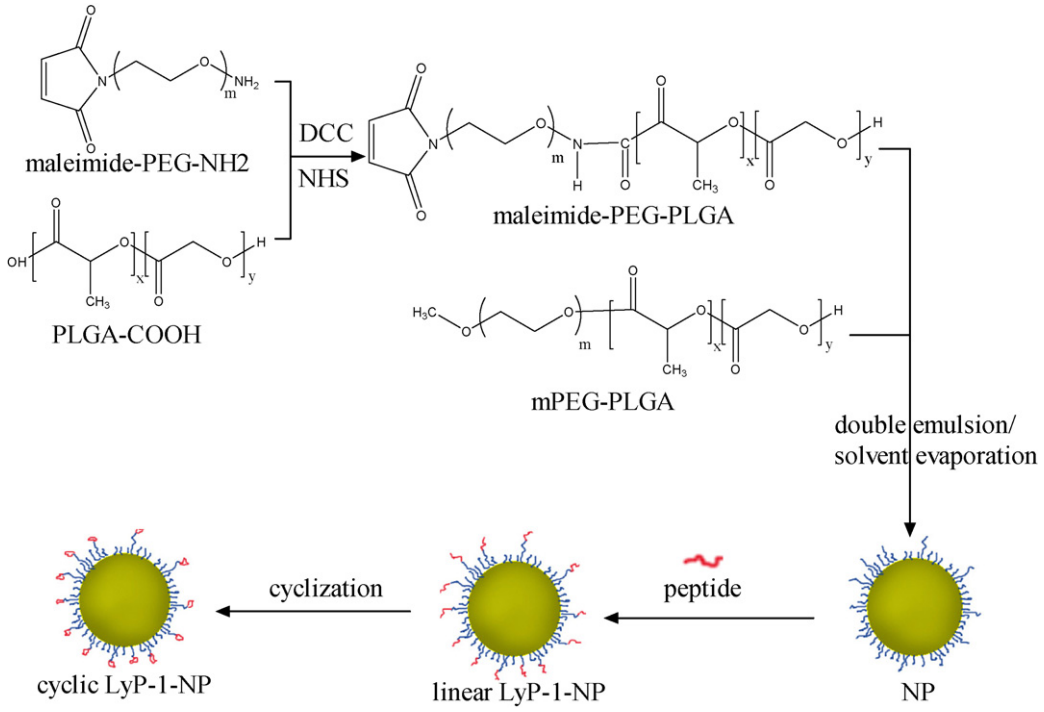

Fig. 1. The schematic diagram of synthesis of LyP-1-NPs. Copolymers of maleimide–PEG–PLGA were synthesized by means of condensation reaction of maleimide–PEG–NH_2 and PLGA–COOH; the pegylated nanoparticles were prepared by the blend of maleimide–PEG–PLGA and mPEG–PLGA using emulsion/solvent evaporation technique; LyP-1 peptide was conjugated with the pegylated nanoparticles through mild stirring with reaction of the thiol and the maleimide groups; cyclization of conjugated LyP-1 peptides was formed by Acm deprotection at C2 and C10 using iodine reagent.

To examine the binding affinity of cyclic LyP-1 to BxPC-3 cells, FITC-labeled peptides at different concentrations (0.01, 0.1, 1, 10 and 100 μmol/L) were directly added to BxPC-3 cells. Blank Cells and cells incubated with 1 mg/mL FITC were used as control. Two hours later, cells were collected. FITC positive cells were observed by fluorescence microscopy (Estativo Eclipse TE 2000S, Nikon, Spain) and analyzed using a FACScan flow cytometer (FACSCalibur, Becton-Dickinson, America) to measure fluorescence (494 nm excitation, 518 nm emission). For cytometer analyzing, a total of at least 10,000-gated events were obtained for each sample.

2.4. Preparation of maleimide-PEG–PLGA

Copolymer maleimide–PEG–PLGA was synthesized by the conjugation of maleimide–PEG–NH_2 to PLGA–COOH (Cheng et al., 2007). One gram of PLGA–COOH was dissolved in 4 mL dichloromethane and stirred at RT for 4 h in the presence of NHS (1:8 PLGA:NHS molar ratio) and DCC (1:8 PLGA:DCC molar ratio) to form an ester. PLGA-NHS was precipitated with ice-cold ethyl ether (5 mL), and repeatedly washed in an ice-cold mixture of ethyl ether and methanol to remove residual NHS and DCC. Trace solvents were removed under vacuum for 2 h. The polymer was re-dissolved in 4 mL dichloromethane followed by addition of maleimide–PEG–NH_2 (1:1.3 PLGA:PEG molar ratio) and incubated under gentle stirring overnight with DIPEA (28 mg, 0.22 mmol). The polymer was washed with ice-cold methanol to remove unreacted PEG. The final maleimide–PEG–PLGA product was recovered using ethyl ether, vacuum dried for 2 h, and stored at 4 °C until use. Polymer was dissolved in deuterated chloroform (5–10 mg/mL) in a glass NMR tube and analyzed on a Bruker Avance 500 AV system (Germany) using standard proton NMR to verify maleimide–PEG–NH_2 conjugation to PLGA. The extent of conjugation was quantified.

2.5. Preparation of nanoparticles

Nanoparticles made of a blend of mPEG–PLGA and maleimide–PEG–PLGA were prepared through the emulsion/solvent evaporation technique, similar to previously described (Lu et al., 2005; Olivier et al., 2002). Fifty microliters of water was emulsified by continuous sonication (30 s) on ice using a probe sonicator (JY92-II sonifier cell discruptor, Xinzhi Biotech Co., China) at 160 W in 1 mL of dichloromethane solution containing mPEG–PLGA and maleimide–PEG–PLGA at a certain ratio (total amount: 30 mg). This primary emulsion was then intermissively emulsified by sonication (30 s) at 160 W on ice in 2 mL of a 1% sodium cholate aqueous solution. The w/o/w emulsion obtained was diluted into 38 mL of a 0.5% sodium cholate aqueous solution under rapid magnetic stirring. After 10 min, dichloromethane was evaporated under vacuum and at 40 °C using a Buchi Rotavapor R-200 and Heating Bath B-490 (Germany). Nanoparticles were then centrifuged at 14,000 rpm with a TJ-25 Beckman Coulter TM Centrifuge equipped with AT-14-50 rotor (USA) at 4 °C for 45 min. After discarding the supernatant, they were re-suspended in a minimal volume of water and stored at 4 °C until use. The preparation of nanoparticles loaded with 6-coumarin was the same as that of nanoparticles without 6-coumarin, except that 15 μL 6-coumarin (1 mg/mL stock solution in dichloromethane) was additionally added to dichloromethane containing copolymers before primary emulsification.

2.6. Preparation of LyP-1-NPs

LyP-1 with sulfhydryl group was conjugated to the maleimide function located at the distal end of PEG surrounding the nanoparticle surface. LyP-1 was mixed with nanoparticles at a peptide:maleimide ratio of 1.3:1 in PBS (pH 7.0). The volume of mixture was 1 mL and the conjugation of LyP-1 to maleimide on the nanoparticles was performed overnight on a rotating plate set at a low speed (Lu et al., 2005). Nanoparticles were concentrated by centrifuging at 14,000 rpm at 4 °C for 45 min.

Cyclization of conjugated LyP-1 was performed by Acm deprotection at Cys^2 and Cys^{10} using iodine reagent. Nanoparticles were mixed with 0.2 mol/L citric acid at a concentration of 1 mg/mL. One-tenth volume of 1 mol/L hydrochloride was added to the mixture. Iodic methanol solution (5 mmol/L) was immediately added at a peptide:iodine molar ratio of 1:1 and stirred at RT for 1 h. Ascorbic acid (1 mol/L) was dropped into the solution until the color of mixture became clear. Nanoparticles were collected by centrifuging at 14,000 rpm at 4 °C for 45 min. In order to examine the conjugation efficiency of LyP-1 to maleimide on the nanoparticles, maleimide–PEG–PLGA and mPEG–PLGA nanoparticles were incubated at RT with LyP-1 presence (+) or absence (−) of FITC to conjugate. Fluorescence intensity of FITC-labeled nanoparticles was quantified by spectrofluorometry (LS 50B luminescence spectrometer, Perkin-Elmer).

2.7. Nanoparticles characterization

The mean (number based) diameter and zeta potential of the nanoparticles were determined by dynamic light scattering using a Zeta Potential/Particle Sizer NICOMP TM 380 ZLS (PSS.NICOMP Particle Size System, Santa Barbara, USA) at 25 °C and at a scattering angle of 90° at a concentration of approximately 1 mg nanoparticle/mL water. The morphology of LyP-1-NPs was observed by transmission electron microscope (TEM, JEM-2010/INCA Oxford, JEOL, Japan) and scanning electron microscope (SEM, FEI SIRION 200/INCA Oxford, America). The influences of mPEG–PLGA/maleimide–PEG–PLGA ratio and peptide cyclization procedure on nanoparticle morphology were also examined.

2.8. Cellular uptake of LyP-1-NPs

BxPC-3 cells were cultured in RPMI-1640 medium supplemented with 10% fetal bovine serum and maintained at 37 °C in a 5% CO_2 humidified atmosphere. Media was changed every 48 h, and cells were passaged with EDTA–trypsin when confluent. In order to examine the active targeting effect of LyP-1-NPs to pancreatic cancer cells, 6-coumarin loaded LyP-1-NPs (0.5 mg/mL) were added to BxPC-3 cells. Blank Cells and cells treating with NPs (0.5 mg/mL) were used as control. To detect the interference effect of LyP-1 to LyP-1-NPs cellular internalization, LyP-1-NPs were added to BxPC-3 cells pretreated with 1 μmol/L LyP-1. Twenty-four hours after incubating with nanoparticles, fluorescence positive cells were examined by FACScan flow cytometer as described in Section 2.2.

2.9. In vivo tracking of nanoparticles

Nude BALB/c nu/nu mice received subcutaneous injection of 1×10^6 BxPC-3 cells via nail pad to induce lymphatic metastasis tumor models (Yang et al., 2009). Three weeks after inoculation, these mice received either 6-coumarin loaded LyP-1-NPs or 6-coumarin loaded NPs as a control (3 per group) via the nail pad at a dose of 60 mg/kg body weight. Twelve hours post-administration, animals were sacrificed, and the popliteal, inguinal, iliac and renal hilus lymph nodes were harvested to examine the lymphatic distribution of these particles. Metastasis lymph nodes were confirmed by hematoxylin eosin (H&E) staining and pathological examination. Nanoparticles distributing in the lymph nodes were observed by a living imaging system (GE explore, USA) using UV (6-coumarin) filter. The 6-coumarin positive cells from the lymph nodes were quantified by flow cytometer to measure fluorescence as described above.

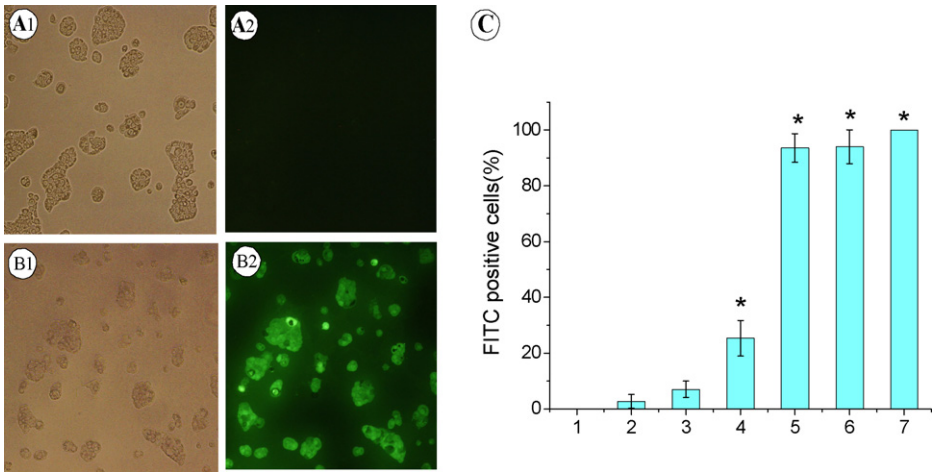

Fig. 2. Binding capacity of FITC-labeled LyP-1 to BxPC-3 cells. No obvious FITC fluorescence was detected by microscopy when cells were incubated with 1 mg/mL FITC (A1 and A2), and nearly all the cells were stained with green fluorescence when cells were incubated with 10 μmol/L FITC-labeled LyP-1 (B1 and B2). The FITC positive cells were quantified by flow cytometer at different concentrations of FITC-labeled LyP-1 (C). Results were expressed as percentage of total cells and data were given as mean ± SD. 1, Blank, 2, 1 mg/mL FITC, 3, 0.01 μmol/L LyP-1-FITC, 4, 0.1 μmol/L LyP-1-FITC, 5, 1 μmol/L LyP-1-FITC, 6, 10 μmol/L LyP-1-FITC, 7, 100 μmol/L LyP-1-FITC (*$p < 0.05$ vs. 2).

2.10. Statistics

Results were summarized as mean ± SD. A Student's *t*-test was used for all statistical analysis between two groups, unless otherwise indicated. A *p*-value of less than 0.05 was considered as statistically significant.

3. Results and discussion

3.1. Examination of LyP-1s binding affinity to BxPC-3 cells

LyP-1 can recognize specific marker molecules on the surface of tumor lymphatic endothelial cells and home to tumor lymphatics and strongly accumulate in cancer xenografts and their metastases (Laakkonen et al., 2002, 2004). However, the homing of Lyp-1 is tumor type-specific, despite the fact that nearly all tumors have been shown to contain lymphatic vessels (Laakkonen et al., 2008). In addition to the MDA-MB-435 tumors, it homes to a transgenic prostate tumor (TRAMP), transgenic breast carcinoma (MMTVPyMT), and to a lesser extent KRIB osteosarcoma xenografts, but not to C8161 melanoma, HL-60 leukemia (Laakkonen et al., 2002) and K14-HPV16/E2 cervical cancer (Zhang et al., 2006).

In this study, the binding affinity of cyclic LyP-1 was examined by being labeled with FITC. Different concentrations of FITC-labeled LyP-1 were incubated with BxPC-3 cells. We found great binding affinity of LyP-1 to BxPC-3 cells at the concentration of 0.1 μmol/L (Fig. 2A1, A2, B1, B2 and C). Furthermore, LyP-1 became internalized by the cells it bonded to, and accumulated in the nucleus of the cells, which indicates LyP-1 is a cell-penetrating peptide (Fig. 2B2) (Laakkonen et al., 2002, 2004).

3.2. Maleimide–PEG–PLGA NMR characterization

We prepared maleimide–PEG–PLGA polymers by a one-step synthesis conducted in anhydrous organic solvents. Bifunctional PEG containing a maleimide group at one terminus and an amino group at the other was used to form maleimide–PEG–PLGA. Proton NMR revealed characteristic peaks of PLGA at 1.5, 4.8 and 5.2 ppm in all PLGA dissolved polymer samples (Fig. 3). Peaks were observed at 6.7, 3.6, 2.2 ppm in maleimide–PEG–NH_2, corresponding to the proton NMR spectra of maleimide–PEG–NH_2 (Fig. 3). Using the integration of the relative molecular weights and peaks, the conjugation efficiency of maleimide–NH_2–PEG to PLGA–COOH was estimated to be approximately 35%.

3.3. LyP-1-NPs preparation and characterization

Nanoparticles were prepared by the blend of maleimide–PEG–PLGA and mPEG–PLGA copolymers using emulsion/solvent evaporation technique. This technique can encapsulate water-soluble drugs in the internal aqueous phase and oil-soluble drugs in the external oil phase, indicating this biodegradable nanoparticles have the potential of delivering both water- and oil-soluble drugs. The molecular weight of PEG in maleimide–PEG–PLGA was chosen to be higher than that in mPEG–PLGA, so that the maleimide function would protrude from the corona which is available for conjugating LyP-1 to form LyP-1-NPs (Lu et al., 2005).

Size of nanoparticles has great impact on their biodistribution (Calvo et al., 2001; Olivier et al., 2002). For lymphatic targeting system, the size should be controlled under 150 nm in diameter since the gap size among lymphatic endothelial cells is between 30 and 150 nm (Ji, 2006). In this study, most nanoparticles were generally spherical and of regular size. The number based average diameter of nanoparticles was around 90 nm with a SD of 2.7 (Fig. 4A and B, Table 1). There was no statistically significant difference in particle size among nanoparticles conju-

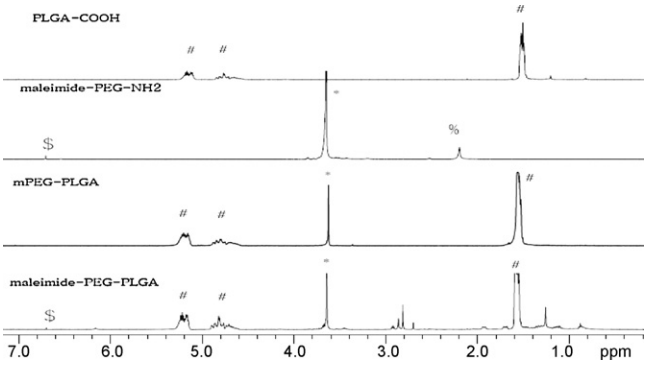

Fig. 3. Proton NMR spectra of PLGA–COOH, maleimide–PEG–NH_2, mPEG–PLGA and maleimide–PEG–PLGA. Polymers were dissolved in deuterated chloroform. Characteristic peaks were visible for PLGA (#), PEG (*), NH_2 (&) and maleimide ($), but not for conjugated peptide linkage.

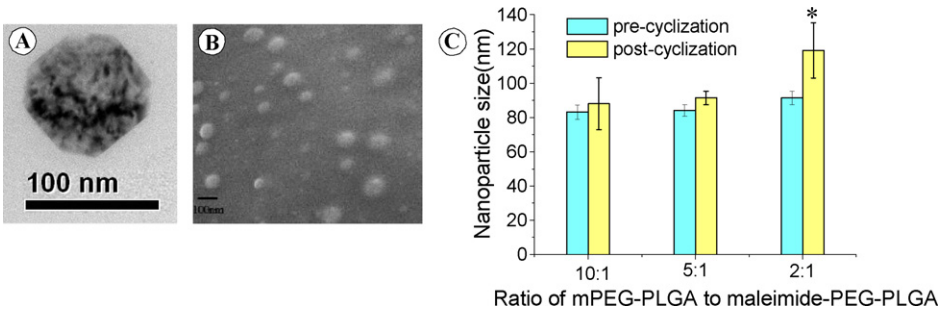

Fig. 4. Characterization of nanoparticles. (A) Transmission electron micrograph of LyP-1-NPs; (B) scanning electron microscopy of LyP-1-NPs; (C) nanoparticles' size pre- and post-cyclization at different molar ratio of mPEG–PLGA to maleimide–PEG–PLGA. The data were given as mean ± SD (*$p < 0.05$ vs. pre-cyclization).

Table 1
Mean particle size, polydispersity index (PI), zeta potential of NPs and LyP-1-NPs loaded or not with 6-coumarin ($n = 3$).

Nanoparticles	Mean size (mean ± SD, nm)	Polydispersity index	Zeta potential (mV)[a]
NPs	83.1 ± 2.7	0.073 ± 0.005	−10.14 ± 1.31
LyP-1-NPs	87.1 ± 5.4	0.132 ± 0.032	−12.34 ± 0.82
6-Coumarin-loaded NPs	87.8 ± 13.2	0.234 ± 0.044	−20.51 ± 1.79
6-Coumarin-loaded LyP-1-NPs NPs NyP-1Ps NPs NPs NPs	91.3 ± 5.4	0.105 ± 0.012	−17.33 ± 1.81

[a] Measured in NaCl solution (10^{-3} M).

gated with LyP-1 and nanoparticles without LyP-1 conjugation, or among those loaded with 6-coumarin and those without 6-coumarin loading, suggesting that neither the conjugation process nor the incorporation of the fluorescent dye influenced the particle size.

In engineering targeted nanoparticles, the tumor-targeting ligand surface density and the antibiofouling surface properties must be balanced (Gu et al., 2008). Increasing the targeted ligand density on nanoparticle surface can increase the rate of nanoparticle uptake *in vitro*. However, the presence of high targeted ligand surface density also leads to an increase in nanoparticle accumulation in the liver and spleen. The OX26-conjugated pegylated nanoparticles showed that the mixture ratio of maleimide–PEG–PLA and mPEG–PLA when preparing nanoparticles was optimized at 1:30 (Olivier et al., 2002). Therefore, we adjusted the mixture ratio of maleimide–PEG–PLGA and mPEG–PLGA to 1:10, and the ratio of LyP-1:maleimide group to 1.3:1 to allow full reaction to the surface maleimide group. No statistically difference was observed before cyclization at different molar ratio of mPEG–PLGA to maleimide–PEG–PLGA.

In this study, cyclic LyP-1 was used since cyclic peptides have been reported to have higher binding affinity and stability than linear ones (Cardarelli et al., 1992). The LyP-1 was synthesized with 10-amino groups containing 3 cysteines, which can be conjugated to the maleimide groups on the nanoparticle surface. The thiol of Cys^2 and Cys^{10} protected by Acm can form cyclic peptide after deprotection. The cyclization process did not show significant impact on the size of nanoparticles when the ratio of mPEG–PLGA to maleimide–PEG–PLGA was below 2:1 (Fig. 4C).

In this study, zeta potentials of 6-coumarin-loaded nanoparticles were lower compared with the blank (Table 1). This can be explained by the fact that the density of PEG "brush" of 6-coumarin-loaded nanoparticles was lower than that of the blank nanoparticles, which was caused by part of PEG chains were embedded inside the matrix when 6-coumarin being entrapped into the nanoparticles (Quellec et al., 1998).

To examine the specific binding efficiency of peptide to maleimide on the surface of nanoparticles, the peptide conjugated to the nanoparticles was labeled by FITC and the fluorescence intensity of FITC-labeled nanoparticles was detected by spectrofluorometry.

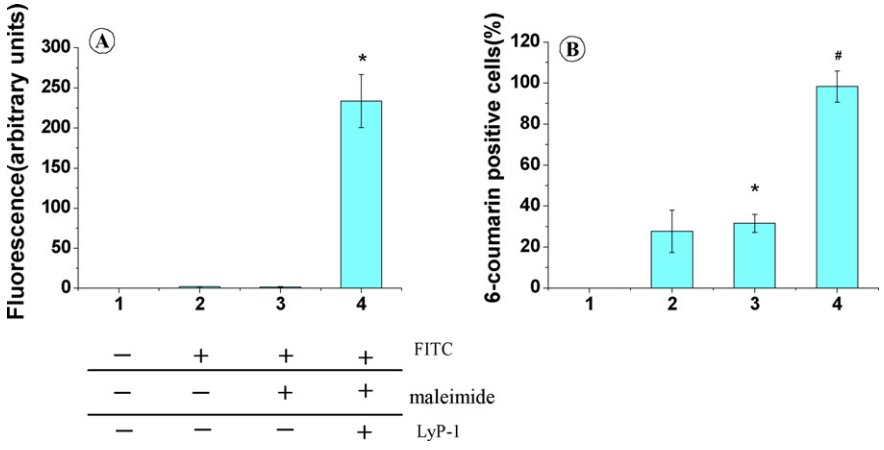

Fig. 5. (A) Specific binding efficiency of LyP-1 to maleimide on nanoparticles. maleimide–PEG–PLGA (+) and mPEG–PLGA (−) nanoparticles were incubated with presence (+) or absence (−) of LyP-1-FITC and the fluorescence intensity of FITC-labeled nanoparticles was detected by spectrofluorometry. The data were given as mean ± SD (*$p < 0.05$ vs. 1, 2, 3). (B) LyP-1-NPs binding affinity to BxPC-3 cells. Cells were treated with 6-coumarin labeled nanoparticles and 6-coumarin positive cells were quantified by flow cytometer. The results were expressed as percentage of total cells and data were given as mean ± SD. 1, Blank, 2, 0.5 mg/mL NPs, 3, 0.5 mg/mL LyP-1-NPs pretreated with 1 μmol/L LyP-1, 4, 0.5 mg/mL LyP-1-NPs (#$p < 0.05$ vs. 2; *$p > 0.05$ vs. 2).

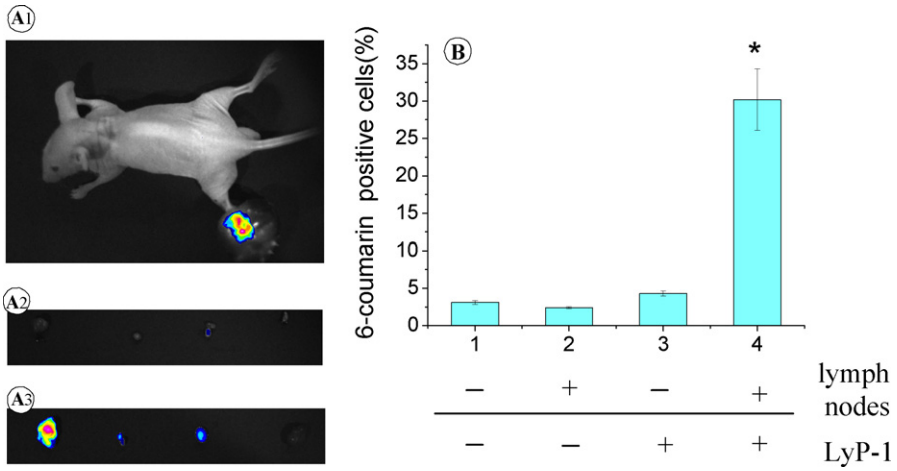

Fig. 6. LyP-1-NPs' binding affinity to metastasis lymph nodes. Nude BALB/c nu/nu mice were injected into the nail pad with 1×10^6 BxPC-3 cells to induce lymphatic metastasis models for 3 weeks (A1). Mice received 6-coumarin loaded NPs (A2) or 6-coumarin loaded LyP-1-NPs (A3) via the nail pad at a dose of 60 mg/kg body weight. After 12 h, animals were sacrificed, and popliteal, inguinal, iliac, and renal hilus lymph nodes were taken out. Nanoparticles distributing in the lymph nodes were observed by a living imaging system (A1 and A2) using UV (6-coumarin) filter. The presence of 6-coumarin in lymph nodes with metastasis (+) or without metastasis (−) was quantified by flow cytometer (B). The results were expressed as percentage of total cells and data were given as mean ± SD ($^*p < 0.05$ vs. 1, 2, 3).

orometry. The fluorescence intensity of specific binding was about 200 times higher compared with non-specific binding (Fig. 5A).

3.4. *In vitro and in vivo nanoparticles internalization*

Currently, nanoparticles formulated with PLGA–PEG block copolymer is being extensively investigated (Cheng et al., 2007; Farokhzad et al., 2006; Garinot et al., 2007; Gu et al., 2008; Townsend et al., 2007). PLGA, FDA-approved biodegradable and biocompatible polymers, have been one of the most extensively investigated biodegradable colloidal drug carriers (Langer, 2001). Surface PEG modification enables the nanoparticles to escape from the arrest of mononuclear phagocytic system (MPS) so as to prolong their half-life in plasma and increase the area under the concentration–time curve (AUC) (Pepinsky et al., 2001). The functionalization of polymer end groups and subsequent conjugation of targeting moieties (peptides, aptamers, and proteins), permit local drug delivery, which could enhance local drug concentration and reduce systemic toxicity (Huynh et al., 2006; Zhang et al., 2008).

Lymphatic vasculature constitutes a second vascular system of tissues, which comprises a network of vessels that unidirectionally transport interstitial fluid and macromolecules back to the blood circulation from the tissues (Saharinen et al., 2004). Tumor lymphatic vasculature carries specific molecular markers, which indicates the possibility of targeting drug delivery to metastatic lesions (Alitalo et al., 2005). Peptide LyP-1 can strongly accumulate in cancer xenografts and their metastases, indicating that LyP-1-NPs have the potential to target both primary tumor lesions and metastasis focuses (Laakkonen et al., 2002, 2004, 2008). Furthermore, LyP-1 also shows anti-cancer effect which can induce death of cells that bind and internalize the peptide (Laakkonen et al., 2004). Systemic LyP-1 treatment of mice with xenografted tumors can inhibit tumor growth (Laakkonen et al., 2004).

The ability of LyP-1 to serving as a targeting peptide for specific nanoparticle delivery to tumor cells was tested. 6-coumarin loaded NPs and LyP-1-NPs were added to BxPC-3 cells. Green fluorescence stained cells were analyzed by flow cytometry. Cellular uptake of LyP-1-NPs was about four times of that of NPs (Fig. 5B). To examine the interference effects of LyP-1 to LyP-1-NPs internalization, cells were pretreated with LyP-1 before adding LyP-1-NPs, which showed great decrease of LyP-1-NPs internalization (Fig. 5B). These results indicated the active targeting role of LyP-1 in LyP-1-NPs to BxPC-3 cells.

To investigate whether this lymphatic metastatic drug delivery system was effective *in vivo*, the existence of nanoparticles loaded with 6-coumarin in the lymph nodes was examined by living imaging system (Fig. 6A1, A2 and A3) and flow cytometry (Fig. 6B). Mice were treated with NPs and LyP-1-NPs via the nail pad (Fig. 6A1). The tumor metastases of all the lymph nodes were determined by H&E staining pathological examination. The distribution of LyP-1-NPs in the metastatic lymph nodes was significantly higher (about eight times) than the non-specific distribution, indicating the potential of this targeting drug delivery system for lymphatic metastatic tumors (Fig. 6A2, A3 and B).

In our experiment, the efficiency of active targeting *in vivo* was better than *in vitro*. This may be explained by the fact that most of the nanoparticles without active targeting ligands were cleared by the circulatory phagocytic system, which did not exist *in vitro*. On the other hand, in the case of active targeting nanoparticles *in vivo*, the specific and selective binding of ligand to its receptor determined the biodistribution of anti-cancer drugs and hence exerted control over pharmacokinetic properties of the drug (Agarwal et al., 2008).

There is a history of using nondegradable and biodegradable nanoparticles for lymphatic targeting (Nishioka and Yoshino, 2001). Compared with other carriers such as liposome and nanotubes used as lymphatics targeting drug delivery, PEG-PLGA nanoparticles possess the benefits of degradability, low toxicity, high efficiency and long circulation time (Cheng et al., 2007; Farokhzad et al., 2006; Garinot et al., 2007; Gu et al., 2008; Townsend et al., 2007). In this experiment, LyP-1 was initially conjugated to biodegradable polymers for targeting lymphatic metastatic tumors and LyP-1-NPs showed a high targeting efficiency both *in vitro* and *in vivo*. In conclusion, LyP-1-NP is a promising carrier for target-specific drug delivery to lymphatic metastatic tumors.

4. Conclusions

Because of the determining role of lymphatic metastasis on the prognosis of cancer patients, targeting drug delivery to lymphatic metastatic tumors is an area of significant research interest. In this study, we developed biodegradable nanoparticles from mPEG–PLGA and maleimide–PEG–PLGA polymers and used them as drug carriers to lymphatic metastatic tumors. LyP-1, which is well-known for its highly specific tumor and tumor lymphatics

targeting, was firstly conjugated to biodegradable polymers for lymphatic metastatic tumors targeting. The LyP-1-NPs showed great targeting efficiency to cancer cells *in vitro* and metastatic focuses *in vivo*. Given the importance of the lymphatic route in metastasis, this delivery system may have great potential for targeting delivery of various therapeutic agents to tumors and their metastatic lymph nodes.

Acknowledgments

This work was supported by the National Natural Science Foundation of China (30500490) and Opening Foundation of Institute of Biomedical Sciences, Fudan University. We thank Dr. Cao Xie for expert technical assistance.

References

Agarwal, A., Saraf, S., Asthana, A., Gupta, U., Gajbhiye, V., Jain, N.K., 2008. Ligand based dendritic systems for tumor targeting. Int. J. Pharm. 350, 3–13.

Alitalo, K., Tammela, T., Petrova, T.V., 2005. Lymphangiogenesis in development and human disease. Nature 438, 946–953.

Brannon-Peppas, L., Blanchette, J.O., 2004. Nanoparticle and targeted systems for cancer therapy. Adv. Drug Deliv. Rev. 56, 1649–1659.

Calvo, P., Gouritin, B., Chacun, H., Desmaele, D., D'Angelo, J., Noel, J.P., Georgin, D., Fattal, E., Andreux, J.P., Couvreur, P., 2001. Long-circulating PEGylated polycyanoacrylate nanoparticles as new drug carrier for brain delivery. Pharm. Res. 18, 1157–1166.

Cardarelli, P.M., Yamagata, S., Taguchi, I., Gorcsan, F., Chiang, S.L., Lobl, T., 1992. The collagen receptor alpha 2 beta 1, from MG-63 and HT1080 cells, interacts with a cyclic RGD peptide. J. Biol. Chem. 267, 23159–23164.

Cheng, J., Teply, B.A., Sherifi, I., Sung, J., Luther, G., Gu, F.X., Levy-Nissenbaum, E., Radovic-Moreno, A.F., Langer, R., Farokhzad, O.C., 2007. Formulation of functionalized PLGA–PEG nanoparticles for in vivo targeted drug delivery. Biomaterials 28, 869–876.

Farokhzad, O.C., Cheng, J., Teply, B.A., Sherifi, I., Jon, S., Kantoff, P.W., Richie, J.P., Langer, R., 2006. Targeted nanoparticle–aptamer bioconjugates for cancer chemotherapy in vivo. Proc. Natl. Acad. Sci. U.S.A. 103, 6315–6320.

Garinot, M., Fievez, V., Pourcelle, V., Stoffelbach, F., des Rieux, A., Plapied, L., Theate, I., Freichels, H., Jerome, C., Marchand-Brynaert, J., Schneider, Y.J., Preat, V., 2007. PEGylated PLGA-based nanoparticles targeting M cells for oral vaccination. J. Control. Release 120, 195–204.

Gu, F., Zhang, L., Teply, B.A., Mann, N., Wang, A., Radovic-Moreno, A.F., Langer, R., Farokhzad, O.C., 2008. Precise engineering of targeted nanoparticles by using self-assembled biointegrated block copolymers. Proc. Natl. Acad. Sci. U.S.A. 105, 2586–2591.

Huynh, G.H., Deen, D.F., Szoka Jr., F.C., 2006. Barriers to carrier mediated drug and gene delivery to brain tumors. J. Control. Release 110, 236–259.

Ji, R.C., 2006. Lymphatic endothelial cells, tumor lymphangiogenesis and metastasis: new insights into intratumoral and peritumoral lymphatics. Cancer Metastasis Rev. 25, 677–694.

Laakkonen, P., Akerman, M.E., Biliran, H., Yang, M., Ferrer, F., Karpanen, T., Hoffman, R.M., Ruoslahti, E., 2004. Antitumor activity of a homing peptide that targets tumor lymphatics and tumor cells. Proc. Natl. Acad. Sci. U.S.A. 101, 9381–9386.

Laakkonen, P., Porkka, K., Hoffman, J.A., Ruoslahti, E., 2002. A tumor-homing peptide with a targeting specificity related to lymphatic vessels. Nat. Med. 8, 751–755.

Laakkonen, P., Zhang, L., Ruoslahti, E., 2008. Peptide targeting of tumor lymph vessels. Ann. N.Y. Acad. Sci. 1131, 37–43.

Langer, R., 2001. Drug delivery. Drugs on target. Science 293, 58–59.

Lu, W., Zhang, Y., Tan, Y.Z., Hu, K.L., Jiang, X.G., Fu, S.K., 2005. Cationic albumin-conjugated pegylated nanoparticles as novel drug carrier for brain delivery. J. Control. Release 107, 428–448.

Nishioka, Y., Yoshino, H., 2001. Lymphatic targeting with nanoparticulate system. Adv. Drug Deliv. Rev. 47, 55–64.

Okada, H., Heya, T., Ogawa, Y., Shimamoto, T., 1988. One-month release injectable microcapsules of a luteinizing hormone-releasing hormone agonist (leuprolide acetate) for treating experimental endometriosis in rats. J. Pharmacol. Exp. Ther. 244, 744–750.

Olivier, J.C., Huertas, R., Lee, H.J., Calon, F., Pardridge, W.M., 2002. Synthesis of pegylated immunonanoparticles. Pharm. Res. 19, 1137–1143.

Oussoren, C., Storm, G., 2001. Liposomes to target the lymphatics by subcutaneous administration. Adv. Drug Deliv. Rev. 50, 143–156.

Pepinsky, R.B., LePage, D.J., Gill, A., Chakraborty, A., Vaidyanathan, S., Green, M., Baker, D.P., Whalley, E., Hochman, P.S., Martin, P., 2001. Improved pharmacokinetic properties of a polyethylene glycol-modified form of interferon-beta-1a with preserved in vitro bioactivity. J. Pharmacol. Exp. Ther. 297, 1059–1066.

Pepper, M.S., 2001. Lymphangiogenesis and tumor metastasis: myth or reality? Clin. Cancer Res. 7, 462–468.

Phillips, W.T., Klipper, R., Goins, B., 2000. Novel method of greatly enhanced delivery of liposomes to lymph nodes. J. Pharmacol. Exp. Ther. 295, 309–313.

Quellec, P., Gref, R., Perrin, L., Dellacherie, E., Sommer, F., Verbavatz, J.M., Alonso, M.J., 1998. Protein encapsulation within polyethylene glycol-coated nanospheres. I. Physicochemical characterization. J. Biomed. Mater. Res. 42, 45–54.

Reddy, G.R., Bhojani, M.S., McConville, P., Moody, J., Moffat, B.A., Hall, D.E., Kim, G., Koo, Y.E., Woolliscroft, M.J., Sugai, J.V., Johnson, T.D., Philbert, M.A., Kopelman, R., Rehemtulla, A., Ross, B.D., 2006. Vascular targeted nanoparticles for imaging and treatment of brain tumors. Clin. Cancer Res. 12, 6677–6686.

Saharinen, P., Tammela, T., Karkkainen, M.J., Alitalo, K., 2004. Lymphatic vasculature: development, molecular regulation and role in tumor metastasis and inflammation. Trends Immunol. 25, 387–395.

Soppimath, K.S., Aminabhavi, T.M., Kulkarni, A.R., Rudzinski, W.E., 2001. Biodegradable polymeric nanoparticles as drug delivery devices. J. Control. Release 70, 1–20.

Townsend, S.A., Evrony, G.D., Gu, F.X., Schulz, M.P., Brown Jr., R.H., Langer, R., 2007. Tetanus toxin C fragment-conjugated nanoparticles for targeted drug delivery to neurons. Biomaterials 28, 5176–5184.

Van Trappen, P.O., Pepper, M.S., 2002. Lymphatic dissemination of tumour cells and the formation of micrometastases. Lancet Oncol. 3, 44–52.

Yang, F., Hu, J., Yang, D., Long, J., Luo, G., Jin, C., Yu, X., Xu, J., Wang, C., Ni, Q., Fu, D., 2009. Pilot study of targeting magnetic carbon nanotubes to lymph nodes. Nanomedicine 4, 317–330.

Zhang, L., Giraudo, E., Hoffman, J.A., Hanahan, D., Ruoslahti, E., 2006. Lymphatic zip codes in premalignant lesions and tumors. Cancer Res. 66, 5696–5706.

Zhang, N., Chittasupho, C., Duangrat, C., Siahaan, T.J., Berkland, C., 2008. PLGA nanoparticle–peptide conjugate effectively targets intercellular cell-adhesion molecule-1. Bioconjug. Chem. 19, 145–152.